Coordination Geometries of Solvated Lanthanide(II) Ions: Molecular Structures of the Cationic Species $[(DIME)_3Ln]^{2+}$ (DIME = Diethylene Glycol Dimethyl Ether; Ln^{2+} = Sm, Yb), $[(DIME)_2Yb(CH_3CN)_2]^{2+}$, $[(DIME)Yb(CH_3CN)_5]^{2+}$, and $[(C_5H_5N)_5Yb(CH_3CN)_2]^{2+}$

James P. White III, Haibin Deng, Edwin P. Boyd, Judith Gallucci, and Sheldon G. Shore*

Department of Chemistry, The Ohio State University, Columbus, Ohio 43210

Received August 18, 1993®

The first lanthanide(II) cationic species with coordination numbers 7, 8, and 9 have been structurally characterized. Mercury amalgams of the elemental lanthanides (Ln(Hg) where Ln = Sm, Eu, Yb) cleanly reduce $Mn_2(CO)_{10}$ and $Co_2(CO)_8$ in polydentate ethers to $[Mn(CO)_5]^-$ and $[Co(CO)_4]^-$ and are oxidized to solvated Ln(II) cations. In the bidentate ether DME (DME = 1,2-dimethoxyethane), $[(DME)_xSm]^{2+}$ ions show some association with the metal carbonylate ions, based upon IR evidence. In the tridentate ether DIME (diethylene glycol dimethyl ether = DIME), IR data suggest that only the solvent-separated species $[(DIME)_3Ln][Co(CO)_4]_2$ (Ln: Sm = 3; Yb = 4) and $[(DIME)_3Ln][Mn(CO)_5]_2$ (Ln: Sm = 5; Yb = 6; Eu = 7) are formed. Structural characterizations confirm the presence of discrete $[(DIME)_3Sm]^{2+}$ and $[(DIME)_3Yb]^{2+}$ ions in **3** and **4**, in which the DIME oxygens form a 9-coordinate tricapped trigonal prismatic geometry about Ln(II). Crystal data for **3**: space group $P6_3$, hexagonal; a = 11.709(2) Å, c = 15.505(3) Å; V = 1841.6 Å^3; Z = 2; at −45 °C; R_F = 0.016 and R_{wF} = 0.020. Crystal data for **4**: space group $P6_3$, hexagonal; a = 11.552(5) Å, c = 15.428(6) Å; V = 1783.1 Å^3; Z = 2; at −60 °C; R_F = 0.066 and R_{wF} = 0.083. The complex ion $[(DIME)_3Sm]^{2+}$ in **3** and **5** and $[(DIME)_3Eu]^{2+}$ in **7** are significantly resistant to air oxidation compared to most other Ln(II) complexes. Insoluble reaction products are formed when $Fe(CO)_5$ is reduced by lanthanide amalgams in ethers. Yb amalgam reductions of $Fe(CO)_5$ in CH_3CN produce the previously characterized $[Hg\{Fe(CO)_4\}_2]^{2-}$ ion, which is isolated as solid $(CH_3CN)_4Yb[Hg\{Fe(CO)_4\}_2]$ (**8**). The complex $(C_5H_5N)_4Yb[Hg\{Fe(CO)_4\}_2]$ (**9**) is isolated from a solution of **8** in C_5H_5N. The mixed-ligand complex $[(C_5H_5N)_5Yb(CH_3CN)_2][Hg\{Fe(CO)_4\}_2]\cdot 2C_5H_5N$ (**10**) crystallizes from a cooled C_5H_5N/CH_3CN solution containing **9**. The cation of **10**, $[(C_5H_5N)_5Yb(CH_3CH)_2]^{2+}$, has pentagonal bipyramidal geometry with the two CH_3CN ligands *trans* on the apexes of the bipyramid. The C_5H_5N ligands form a "five-bladed propeller" configuration along the five equatorial verticies of the bipyramid. Crystal data for **10**: space group $P2_1/m$, monoclinic; a = 12.059(2) Å, b = 17.374(3) Å, c = 12.590(2) Å, β = 99.44(2)°; V = 2601.1 Å^3; Z = 2; at −60 °C; R_F = 0.107 and R_{wF} = 0.077. The mixed-ligand complex $[(DIME)_2Yb(CH_3CN)_2][Hg\{Fe(CO)_4\}_2]$ (**11**) crystallized from a cooled $DIME/CH_3CN$ solution containing **8**. The cation of **11**, $[(DIME)_2Yb(CH_3CN)_2]^{2+}$, has an 8-coordinate, distorted square-antiprismatic arrangement of ligands. Crystal data for **11**: space group $P2_12_12_1$, orthorhombic; a = 9.576(5) Å, b = 15.156(3) Å, c = 23.918(5) Å; V = 3471.2 Å^3; Z = 4; at −60 °C; R_F = 0.040 and R_{wF} = 0.053. A metathesis reaction between $(DIME)_xNa_2[B_{12}H_{12}]$ and $(CH_3CN)_xYbCl_2$ in CH_3CN yields the mixed-ligand complex $[(DIME)Yb(CH_3CN)_5][B_{12}H_{12}]$ (**12**). The coordination geometry around $[(DIME)Yb(CH_3CN)_5]^{2+}$ in **12** is similar to that observed in **11**, based on a square antiprism. Crystal data for **12**: space group $P2_1/n$, monoclinic; a = 12.168(2) Å, b = 14.880(2) Å, c = 17.615(3) Å, β = 97.92(2)°; V = 3159.0 Å^3; Z = 4; at −50 °C; R_F = 0.037 and R_{wF} = 0.054.

1. Introduction

We recently reported studies of divalent lanthanides (Sm(II), Yb(II), and Eu(II)) with hydroborate and transition metal carbonylate substrates.[1-4] Our interests focus on forming neutral coordination complexes of divalent lanthanides that can serve as molecular precursors for metal borides and bimetallic films.[3,5a,b] One of the requirements for such precursors is that any other ligands be neutral and be readily removable. Typically, these ligands are ethers or amines; they are generally employed as solvents in the systems studied. We find that there is a window of stability for neutral monomeric complexes, which depends on the type of anions and neutral bases employed.[3]

The hydroborate ions $[BH_4]^-$ and $[B_{10}H_{14}]^{2-}$ in CH_3CN and in C_5H_5N are systems that form complexes with Ln(II). The hydroborate ions bind to the lanthanide cation through Ln–H–B bridge bonds, which are stable in the presence of these solvents. The complexes $(C_5H_5N)_4Yb[BH_4]_2$, $(CH_3CN)_4Yb[BH_4]_2$, and $(CH_3CN)_6Yb[B_{10}H_{14}]$ have been isolated and structurally characterized.[1,3]

When the basicity of the solvent towards Ln(II) is significantly greater than that of the anion, solvent-separated species are formed. While this is commonly observed spectroscopically, structural characterizations of solvent separated species are lacking. There is only one structurally characterized Ln(II) cationic complex, $[(THF)_6Yb]^{2+}$, reported in the literature,[6] although several Ln(III) cationic complexes have been reported.[7,8] In the present report we describe the isolation and characterization of several compounds, which contain the Ln(II) cationic species $[(DIME)_3Ln]^{2+}$ (Ln = Sm, Eu, Yb), CN = 9; $[(DIME)_2Yb(CH_3CN)_2]^{2+}$ and $[(DIME)Yb(CH_3CN)_5]^{2+}$, CN = 8; and $[(C_5H_5N)_5Yb(CH_3CN)_2]^{2+}$, CN = 7. Coordination geometries

® Abstract published in *Advance ACS Abstracts*, April 1, 1994.

(1) White, J. P., III; Deng, H. B.; Shore, S. G. *J. Am. Chem. Soc.* **1989**, *111*, 8946.
(2) Deng, H. B.; Shore, S. G. *J. Am. Chem. Soc.* **1991**, *113*, 8538.
(3) White, J. P., III; Deng, H. B.; Shore, S. G. *Inorg. Chem.* **1991**, *30*, 2337.
(4) White, J. P., III; Shore, S. G. *Inorg. Chem.* **1992**, *31*. 2756.
(5) (a) White, J. P., III. Ph.D. Dissertation, The Ohio State University, Columbus, OH, 1990. (b) Deng, H. Ph.D. Dissertation, The Ohio State University, Columbus, OH, 1991.
(6) Reference 36 in: Manning, M. J.; Knobler, C. B.; Khattar, R.; Hawthorne, M. F. *Inorg. Chem.* **1991**, *30*, 2009.
(7) Beletskaya, I. P.; Voskoboynikov, A. Z.; Chuklanova, E. B.; Gusev, A. I.; Magomedov, G. K. *Metalloorg. Khim.* **1988**, *1*, 1383.
(8) Evans, W. J.; Bloom, I.; Grate, J. W.; Hughes, L. A.; Hunter, W. E.; Atwood, J. L. *Inorg. Chem.* **1985**, *24*, 4620.

0020-1669/94/1333-1685$04.50/0

depend upon the bases employed. Syntheses of the parent compounds and the molecular structures of these Ln(II) cationic complexes are discussed below.

2. Experimental Section

A. General Data. All manipulations were performed under inert atmosphere conditions. Standard vacuum line and inert atmosphere techniques were employed.[9] Acetonitrile (Mallinckrodt) was stirred over P_2O_5 for 10 days before being distilled for use. Pyridine (Fisher) was dried and distilled from Na immediately prior to use. Tetrahydrofuran, THF (Fisher), and 1,2-dimethoxyethane, DME (Aldrich), were dried with CaH_2 and then distilled from a Na/benzophenone solution immediately prior to use. Diethylene glycol dimethyl ether, DIME, was repeatedly distilled from fresh Na until no effervescence was observed. It was distilled once more and then stored in a sealed flask in a drybox prior to use. Hexanes (Baker) were stirred over H_2SO_4 for 2 days, washed with H_2O, dried with CaH_2, and then distilled from Na before use. Ammonia (Matheson) was distilled from Na immediately prior to use. Ammonium chloride (Fisher) was recrystallized from anhydrous methanol and vacuum dried at 120 °C prior to use. $Mn_2(CO)_{10}$ (Strem) and $Co_2(CO)_8$ (Strem) were vacuum sublimed and stored under N_2 prior to use. $Fe(CO)_5$ (Strem) was distilled immediately prior to use. $[(DIME)_xNa_2][B_{12}H_{12}]$ (Callery) was dissolved in THF, filtered, precipitated, and vacuum-dried at 90 °C prior to use. Yb metal (Strem) and Sm metal (Strem) were used as received. A Eu ingot (Strem) was obtained packed in oil. Washing it with hexanes removed the oil. It was then cut into strips weighing approximately 100 mg. Triply distilled mercury (Bethlehem Instruments) was used as received.

The amalgams used in this laboratory were prepared in a slightly different manner than those produced elsewhere.[10] Approximately 1 mmol of lanthanide metal (Ln = Sm, Yb, Eu) was dissolved in *ca.* 10 mL of mercury by stirring the solution at room temperature in a sealed 50-mL reaction flask under N_2 or vacuum. As the metal dissolves, the resulting amalgam, Ln(Hg), wets the vessel walls. The relative ease of amalgam formation is Yb > Eu > Sm. After 3 h, all the metal had dissolved.

$(CH_3CN)_xYbCl_2$ was synthesized from $(NH_4)Cl$ and Yb metal in liquid NH_3, using a modified literature preparation,[11] details of which have been previously reported.[3]

All IR spectra were recorded with 2-cm^{-1} resolution using a Mattson-Polaris FT-IR spectrometer.

Single-crystal X-ray diffraction data were collected with an Enraf-Nonius CAD4 diffractometer. Computations were carried out on PDP 11/44 and DEC Vax station 3100 computers, using the SDP structure determination package.[12] Lattice parameters were determined from 25 reflections distributed in the 2θ range $24 \leq 2\theta \leq 30°$. All data were corrected for Lorentz and polarization effects. An empirical absorption correction (ψ-scans) was also applied for each structure. The lanthanide positions were determined from a Patterson map or by using the direct-methods program MULTAN 11/82. The remaining atoms were located and the structure were solved by a combination of the direct-methods program MULTAN 11/82 and difference Fourier techniques with analytical scattering factors used throughout. Full-matrix least-squares refinements were employed. Hydrogen atoms were calculated at ideal geometries with d(C–H) = 0.95 Å; for a methyl group, one hydrogen atom was found on a difference Fourier map and the positions of the remaining ones were calculated as described above. New hydrogen positions were updated after each refinement of non-hydrogen atoms until convergence. For those structures solved in noncentric space groups (3, 4, and 11), the enantimorphic forms were refined. R values for the enantiomers were significantly different. The structures of the enantiomers with the lower R_F and R_{wF} values are reported.

Elemental analyses of materials were performed by one of two laboratories: Oneida Research Services, Inc., One Halsey Rd., Whitesboro, NY 13492, or Analytische Laboratorien, Fritz-Pregl-Strasse 24, D-5270 Gummersbach 1 Elbach, Germany.

B. $(DME)_xSm[Co(CO)_4]_2$ (1). A 50-mL flask with 5 mL of a Sm amalgam (52.4 mg Sm, 0.348 mmol) is charged with 118 mg of $Co_2(CO)_8$ (0.344 mmol) and a magnetic stir bar in the drybox and sealed with a vacuum line adaptor. The flask is cooled to −78 °C and evacuated, and *ca.* 15 mL of DME is condensed into the flask. The reaction flask is then warmed to room temperature and stirred. A dark green color begins to form immediately upon warming, and the reaction appears to be complete after 30 min by the appearance of mobile mercury. After 2 h, the flask is returned to the drybox, and the solvent is decanted off the mercury layer into a clean 50-mL flask, to which a fine-fritted vacuum line extractor is connected. The extractor is then degassed, and the DME solution is filtered to remove residual amounts of the amalgam present. The filtrate is a red-green solution, which is thermochromic; it exhibits a brilliant emerald green color when cooled below −40 °C, and reverts back to the green–rod color at room temperature. Solution IR, (DME, NaCl plates): ν_{CO} 2032 (w), 2014 (vw), 2004 (vw), 1936 (s), 1888 (vs,s), 1812 (w), 1744 (w), 1709 (vw), 1455 (s) cm^{-1}. Solvent was pumped away at room temperature over a period of *ca.* 12 h leaving a black-purple solid which is a nonstoichiometric material. Anal. Found: C, 27.87; H, 3.27; Co, 14.42; Sm, 18.69. Empirical formula: $(DME)_{2.70}Sm[Co(CO)_4]_{1.98}$.

C. $(DME)_xSm[Mn(CO)_5]_2$ (2). In a procedure similar to that used for 1 above, a 50-mL flask with 8 mL of a Sm amalgam (133 mg Sm, 0.886 mmol) is charged with 345 mg $Mn_2(CO)_{10}$ (0.885 mmol) and reacted in 15 mL of DME to give a dark green solution. Solution IR (DME, NaCl plates): ν_{CO} 2032 (s), 2013 (w), 1969 (s), 1892 (vs,sh), 1866 (vs,sh), 1782 (w) cm^{-1}; ν_{Mn-C} 686 (vs,s), 657 (vs,s) cm^{-1}. Solvent was pumped away at room temperature over a period of *ca.* 12 h leaving a black-purple solid which is a nonstoichiometric material. Anal. Found: C, 30.27; H, 2.85; Mn, 13.52; Sm, 18.71. Empirical formula: $(DME)_{2.61}Sm[Mn(CO)_5]_{1.98}$.

D. $[(DIME)_3Sm][Co(CO)_4]_2$ (3). A 50-mL flask with 7 mL of a Sm amalgam (104 mg Sm, 0.692 mmol) is charged with 194 mg of $Co_2(CO)_8$ (0.566 mmol) and a magnetic stir bar in the drybox. Next *ca.* 10 mL of DIME is pipetted into the flask, which is sealed, degassed, and stirred. A dark red color begins to form as soon as the solvent is added. The reaction appears to be complete after 30 min. After 2 h, the flask is returned to the drybox where the resulting solution is siphoned off the Hg layer and placed into a 50-mL flask, which is connected to a fine-fritted vacuum line extractor. The solution is filtered by partial evacuation of the receiving flask, yielding a deep red filtrate. The excess solvent is removed under vacuum, producing ruby-red crystals. In the drybox, the flask containing the crystals is connected to an extractor which is then evacuated, and *ca.* 10 mL of hexanes are condensed onto the crystals. The crystals are washed twice with hexanes to remove excess solvent and then vacuum dried. Yield: 500 mg (81%) of **3**. Compound **3** is soluble in ethers and CH_3CN and slightly soluble in toluene and $(CH_3)_2S$. Anal. Calcd for $C_{22}H_{42}O_{17}SmCo_2$: C, 34.89; H, 4.73. Found: C, 34.98; H, 4.66. Solution IR (DIME, KBr plates): ν_{CO} 2004 (w), 1886 (vs, br, sh) cm^{-1}; ν_{Co-C} 558 (s), 552 (s) cm^{-1}.

E. $[(DIME)_3Yb][Co(CO)_4]_2$ (4). In a procedure similar to that used to prepare **3**, a 50-mL flask with 15 mL of a Yb amalgam (178 mg Yb, 1.03 mmol) is charged with 342 mg of $Co_2(CO)_8$ (1.00 mmol) and a magnetic stir bar in the drybox. Then 15 mL of DIME is pipetted into the flask. After 6 h of stirring at room temperature, the yellow-green solution is decanted from the Hg layer and filtered. The DIME is removed, and the yellow-tan solid is washed with *ca.* 10 mL of hexanes and dried. Yield: 710 mg (77%) of **4**. Anal. Calcd for $C_{26}H_{42}O_{17}YbCo_2$: C, 34.04; H, 4.61. Found: C, 33.59; H, 4.34. The crystal structure of **4** is isomorphous to that of **3**. The IR spectrum of **4** in solution is identical to that of **3** within experimental error.

F. $[(DIME)_3Sm][Mn(CO)_5]_2$ (5). In a procedure similar to that used to prepare **3**, a 50-mL flask containing 10 mL of a Sm amalgam (110 mg Sm, 0.732 mmol) is charged with 239 mg of $Mn_2(CO)_{10}$ (0.612 mmol) and a magnetic stir bar in the drybox. Then *ca.* 10 mL of DIME is pipeted into the flask, which is sealed, degassed, and stirred at room temperature. The reaction appears to be complete after 30 min. After 2 h, a deep red-orange solution is decanted from the Hg layer and placed in a clean 50-mL flask. The flask is connected to a fine-fritted vacuum line extractor and the solution is filtered. The excess solvent is removed under vacuum, producing red-orange crystals. The flask containing the crystals is connected to a clean extractor in the drybox. The extractor is then evacuated, and *ca.* 10 mL of hexanes are condensed onto the crystals. The crystals are washed twice with hexanes to remove excess solvent and then vacuum dried. Yield: 605 mg (88%) of **5**. Anal. Calcd for $C_{28}H_{42}O_{19}SmMn_2$: C, 35.67; H, 4.49. Found: C, 35.66; H, 4.32.

(9) Shriver, D. F.; Drezdzon, M. A. *The Manipulation of Air Sensitive Compounds*, John Wiley & Sons: New York, 1969.
(10) Suleimanov, G. Z.; Rybakova, L. F.; Nuriev, Ya. A.; Kurbanov, T. Kh.; Beletskaya, I. P. *J. Organomet. Chem.* **1982**, *235*, C19.
(11) Howell, J. K.; Pytlewski, L. L. *J. Less Common Met.* **1969**, *18*, 437.
(12) SDP (Developed by B. A. Frenz and Associates, Inc., College Station TX 77840) was used to process X-ray data, to apply corrections, and to solve and refine the structures.

Solution IR (DIME, KBr plates): ν_{CO} 2012 (vw), 1896 (vs, s) 1863 (vs, s) cm^{-1}; ν_{Co-C} 686 (s), 659 (s) cm^{-1}. Solid IR (nujol, KBr plates): ν_{CO} 2014 (w), 1927 (vs, br), 1872 (vs, br), 1823 (vs) cm^{-1}; ν_{DIME} 1103 (m), 1090 (s), 1006 (m), 866 (m, s) cm^{-1}; ν_{Co-C} 681 (vs, s), 656 (vs, s) cm^{-1}.

G. $[(DIME)_3Yb][Mn(CO)_5]_2$ (6). In a procedure identical to that used to prepare **3**, a 50-mL flask with 10 mL of a Yb amalgam (106 mg Yb, 0.615 mmol) is charged with 210 mg of $Mn_2(CO)_{10}$ (0.538 mmol) and a magnetic stir bar in the drybox. Then 10 mL of DIME is pipeted into the flask, and the flask is sealed, degassed, and stirred at room temperature. After 2 h, a yellow-green solution is decanted from the Hg layer and filtered. The excess solvent is removed under vacuum, producing yellow-green crystals. The crystals are washed twice with hexanes. Yield: 450 mg (76%) of **6**. Anal. Calcd for $C_{28}H_{42}O_{19}YbMn_2$: C, 34.83; H, 4.38. Found: C, 34.74; H, 4.27. Compound **6** crystallizes in a trigonal lattice. However, the X-ray data yielded no solution, however. Unit cell data for **6** in space group $R3$: $a = 10.059(3)$ Å, $\alpha = 77.93(2)°$, $V = 959(6)$ Å^3. The IR spectra of **6** in solution and as a solid in Nujol are identical with those of **5** within experimental error.

H. $[(DIME)_3Eu][Mn(CO)_5]_2$ (7). In a procedure identical to that used to prepare **3**, a 50-mL flask with 10 mL of an Eu amalgam (93.5 mg Eu, 0.615 mmol) is charged with 193 mg of $Mn_2(CO)_{10}$ (0.495 mmol) and a magnetic stir bar in the drybox. Then 10 mL of DIME is pipetted into the flask, and the flask is sealed, degassed, and stirred at room temperature. After 2 h, a light yellow solution is decanted from the Hg layer and filtered. The excess solvent is removed under vacuum, producing yellow crystals. The crystals are washed twice with hexanes. Yield: 440 mg (85%) of **7**. Anal. Calcd for $C_{28}H_{42}O_{19}EuMn_2$: C, 35.61; H, 4.48. Found: C, 35.84; H, 4.46. The IR spectra of **7** in solution and as a solid in Nujol are identical with those of **5** and **6** within experimental error.

I. $(CH_3CN)_4Yb[Hg\{Fe(CO)_4\}_2]$ (8). A 50-mL flask containing 15 mL of a Yb amalgam (200 mg Yb, 1.16 mmol) is evacuated, and 20 mL of dry CH_3CN and 0.30 mL (2.3 mmol) of $Fe(CO)_5$ are distilled into the vessel at −78 °C. The mixture is stirred at room temperature for 30 min and then cooled to −78 °C, and CO is pumped away. The reaction flask is warmed to room temperature and stirred for another 2 h, after which the flask is cooled to −78 °C and CO gas is again removed. The flask is again warmed and stirred for an additional 3 h at room temperature. The resulting suspension is next decanted from Hg into a 50-mL flask in a drybox, which is connected to a fine-fritted vacuum line extractor. The solution is filtered and CH_3CN solvent is removed from the filtrate under vacuum. The resulting yellow solid is washed with *ca.* 10 mL of hexanes and dried under vacuum. Yield: 635 mg (64%) of **8**. Anal. Calcd for $C_{16}H_{12}Fe_2HgN_4O_8Yb$: C, 22.00; H, 1.38; N, 6.41. Found: C, 21.78; H, 1.26; N, 6.09. Solid IR (Nujol, NaCl plates): ν_{CO} 2036 (w), 1990 (m, sh), 1945 (s, sh), 1937 (s), 1876 (s), 1839 (s), 1815 (s); ν_{CN} 2302 (w, sh), 2298 (w), 2273 (w, sh), 2270 (w) cm^{-1}. Solution IR (CH_3CN, NaCl plates): ν_{CO} 2023(m), 1990 (m, sh), 1974 (s), 1934 (m), 1919 (m), 1870 (vs, br) cm^{-1}.

J. $(C_5H_5N)_4Yb[Hg\{Fe(CO)_4\}_2]$ (9). Complex **8** is dissolved in *ca.* 15 mL of pyridine, and then the solvent is slowly pumped away under vacuum at room temperature. Anal. Calcd for $C_{28}H_{20}Fe_2HgN_4O_8Yb$: C, 32.78; H, 1.97; N, 5.46. Found: C, 33.41; H, 2.06; N, 5.94. Solid IR (Nujol, NaCl plates): ν_{CO} 2025 (w), 1939 (s), 1867 (s), 1760 (s); $\nu_{C=C}$ 1600 (w) cm^{-1}. Its solution IR spectrum is similar to that of **8**. Solution IR (CH_3CN, NaCl plates): ν_{CO} 2022 (w), 2005 (vw), 1973 (s), 1939 (m, sh), 1917 (m), 1880 (s). Very thin needles of $(C_5H_5N)_xYb[Hg\{Fe(CO)_4\}_2]$ (red) were grown by cooling a saturated pyridine solution of **9** to −30 °C for 1 week. However, the needles proved to be too thin for X-ray diffraction studies.

K. $[(C_5H_5N)_5Yb(CH_3CN)_2][Hg\{Fe(CO)_4\}_2]\cdot 2C_5H_5N$ (10). The crystals of **9** obtained from the saturated pyridine solution at −30 °C, described above, are dissolved in a minimal amount of CH_3CN, and the saturated solution is cooled to −40 °C for one week. Red platelike crystals of **10** grow from the solution. Solution IR (CH_3CN, NaCl plates): 2022 (w), 1972 (m), 1939 (s), 1920 (m, sh), 1860 (vs) cm^{-1}. The structure of **10** was determined by single-crystal X-ray analysis. When **10** is dried under vacuum at room temperature, it is converted to **9**, quantitatively.

L. $[(DIME)_2Yb(CH_3CN)_2][Hg\{Fe(CO)_4\}_2]$ (11). Complex **8** is dissolved in a minimal amount of a 1:1 DIME/CH_3CN. The saturated solution is cooled to −40 °C for 2 weeks and yellow crystals of **11** appear. Its solution IR spectrum is similar to that of **8**. The structure of **11** was determined by single-crystal X-ray analysis. The crystals decompose at room temperature.

M. $[(DIME)Yb(CH_3CN)_5][B_{12}H_{12}]$ (12). In a drybox a 50-mL flask containing 1.21 mmol of $(CH_3CN)_xYbCl_2$ (derived from 210 mg of Yb metal, 1.21 mmol) is charged with 375 mg of $(DIME)_xNa_2[B_{12}H_{12}]$ (*ca.* 1.2 mmol for $x = 1$) and a magnetic stir bar. The flask is attached to a fine-fritted vacuum line extractor and evacuated. Next, 20 mL of CH_3CN is condensed into the flask at −78 °C, and the mixture is warmed to room temperature and stirred. The color quickly turns yellow-orange as the flask warms. The solution is stirred for 8 h, after which a yellow-orange suspension is observed. The mixture is filtered, separating into a yellow and white solid and a bright yellow-orange filtrate. Cooling the filtrate to 0 °C with slow removal of the solvent under vacuum produces yellow orange crystals of **12**. The crystals decompose *via* loss of CH_3CN in a dry atmosphere or in vacuum at room temperature. The structure of **12** was determined by single-crystal X-ray analysis.

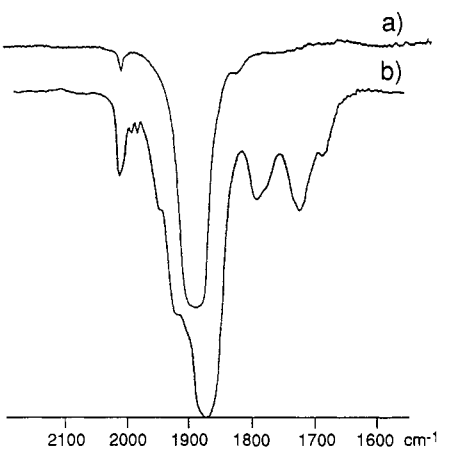

Figure 1. Solution IR spectra of (a) $[(DIME)_3Sm][Co(CO)_4]_2$ (**3**) in DIME and (b) $(DME)_xSm[Co(CO)_4]_2$ (**1**) in DME.

3. Results and Discussion

A. Reduction of $Co_2(CO)_8$ and $Mn_2(CO)_{10}$ by Lanthanide Amalgams in DME and DIME. Lanthanide amalgams in the bidentate and tridentate ethers DME and DIME cleanly reduce $Co_2(CO)_8$ and $Mn_2(CO)_{10}$ (reactions 1–4).[13] When $Co_2(CO)_8$

$$Ln(Hg) + Co_2(CO)_8 \xrightarrow{DME} [(DME)_xLn][Co(CO)_4]_2 \quad (1)$$
Ln: Sm = **1**

$$Ln(Hg) + Mn_2(CO)_{10} \xrightarrow{DME} [(DME)_xLn][Mn(CO)_5]_2 \quad (2)$$
Ln: Sm = **2**

$$Ln(Hg) + Co_2(CO)_8 \xrightarrow{DIME} [(DIME)_3Ln][Co(CO)_4]_2 \quad (3)$$
Ln: Sm = **3**; Yb = **4**

$$Ln(Hg) + Mn_2(CO)_{10} \xrightarrow{DIME} [(DIME)_3Ln][Mn(CO)_5]_2 \quad (4)$$
Ln: Sm = **5**; Yb = **6**; Eu = **7**

is reduced by Sm(Hg) in DME, a green–red, thermochromic solution of **1** is formed which reversibly changes to an emerald-green color below −40 °C. However, when the reduction is carried out in DIME a ruby-red solution of **3** is formed that is not thermochromic. The IR spectrum of the DIME solution of **3** in the ν_{CO} region (Figure 1a) shows absorptions that are nearly identical with those observed for alkali metal salts of $[Co(CO)_4]^-$ in ethers, where it exists as a solvent-separated anion.[14] Also, the X-ray crystal structure of **3** contains $[Co(CO)_4]^-$ ions that are not associated with the Sm(II) cation. While the strongest IR

(13) An earlier brief report states that reaction of Sm and Yb amalgams with $Co_2(CO)_8$ and $Mn_2(CO)_8$ in THF produces $Ln(THF)_x[Co(CO)_4]_3$ and $Ln(THF)_x[Mn(CO)_5]_3$. Suleimanov, G. Z.; Rybakova, L. F.; Abullaeva, L. T.; Paeynskii, A. A.; Beletskaya, I. P. *Dokl. Akad. Nauk SSSR* **1983**, *272*, 885.

(14) Edgell, W. F.; Lyford, J.; Wright, R.; Risen, W. M., Jr.; Watts, A. T. *J. Am. Chem. Soc.* **1970**, *92*, 2240.

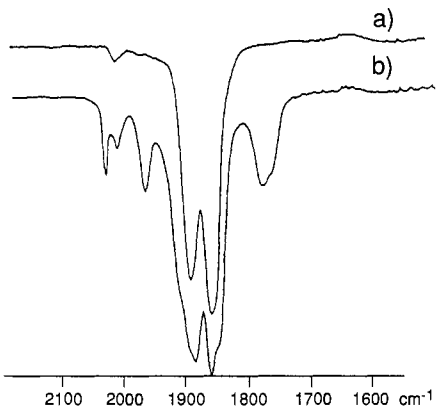

Figure 2. Solution IR spectra of (a) $[(DIME)_3Sm][Mn(CO)_5]_2$ (**5**) in DIME and (b) $(DME)_xSm[Mn(CO)_5]_2$ (**2**) in DME.

Scheme 1

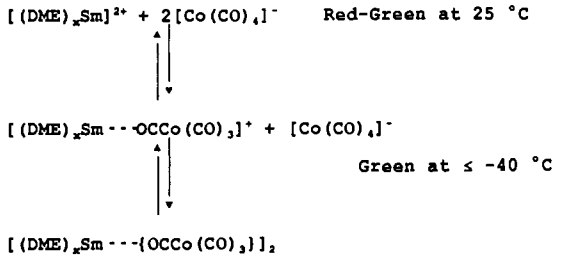

absorption in the room temperature DME solution spectrum of **1** is the single band attributable to free $[Co(CO)_4]^-$ (Figure 1b), additional absorptions in the ν_{CO} region indicate the presence of lower symmetry $[Co(CO)_4]^-$ as well. Such symmetry reduction could be due to bonding of the carbonylate anion to Sm(II), possibly through an isocarbonyl linkage. It is believed that an equilibrium mixture of species exists in the DME solutions: a solvent-separated DME complex as the principal species at room temperature and a complex with the carbonylate ion coordinated to the Sm(II) cation.

The thermochromism of the DME solution of **1** is attributed to temperature dependence of the concentrations of the species in equilibrium (Scheme 1). At low temperature, the inner sphere complex(es) would be more stable, resulting in these species forming principally and giving the resulting emerald-green color. As the temperature is raised, the solvent is better able to displace the carbonylate ion from the Sm(II) coordination sphere, shifting the equilibrium in favor of the solvent-separated species. The presence of both species would account for the green–red color of the solution.

In the DIME solutions, however, the solvent-separated species is apparently so strongly favored that the carbonylate ion does not displace the DIME ligands to any appreciable extent, and the red solvated cation is observed over the temperature range employed.

The DIME solution IR spectrum (Figure 2a) of the Sm(Hg) reductions of $Mn_2(CO)_{10}$ shows only bands attributable to free $[Mn(CO)_5]^-$,[15] while the DME solution IR spectrum (Figure 2b) shows additional bands indicating additional species and/or lower symmetry for the metal carbonyl ligands. The DME solution IR spectrum (room temperature) is also similar to the cobalt carbonylate in that the band for the free carbonylate appears to dominate the spectrum. The equilibrium process proposed for solutions of **1** in DME is also suggested for solutions of **2** in DME.

The stability of the $[(DIME)_3Ln]^{2+}$ cations toward loss of DIME is noteworthy. Compounds **3**–**7** can be safely dried in vacuum at room temperature without loss of the DIME ligands. This is in contrast to the DME complexes **1** and **2** which are isolated as nonstoichiometric solids with the number of DME's per metal varying between **2** and **3**. Generally monodentate ether and amine ligands are easily pumped away from most Ln(II) ions.

The solid DME complexes **1** and **2** are rapidly oxidized in air, typical for Ln(II) compounds. Of the DIME complexes the Yb(II) derivative, **4**, is rapidly oxidized in air; however, the Sm(II) complexes **3** and **5** and the Eu(II) complex **7** are remarkably resistant to air oxidation. A possible reason for these differences in oxidative stabilities is discussed in Section 3.B.

B. Structures of $[(DIME)_3Ln][Co(CO)_4]_2$ (Ln: Sm = 3; Yb = 4). These structures are isomorphous. Diffraction symmetries indicate a hexagonal unit cell. Systematic absences are consistent with space groups $P6_3$, $P6_3/m$, and $P6_322$. Structures were successfully solved and refined in the space group $P6_3$. All the $[(DIME)_3Ln]^{2+}$ cations and $[Co(CO)_4]^-$ anions reside on 3-fold rotation axes. Non-hydrogen atoms were refined anisotropically. Hydrogen atoms were either located or their positions were calculated.

The structure of **4** was not as well refined as that of **3** due to a poorer data set. The structure of the carbonylate ions in **3** and **4** is identical to that observed for the anion in other salts.[8,16] Crystallographic data for **3** and **4** are given in Table 1. Positional parameters are listed in Tables 2 and 3, and selected bond angles and bond distances are given in Tables 4 and 5. In the molecular

Table 1. Crystallographic Data for $[(DIME)_3Sm][Co(CO)_4]_2$ (**3**) and $[(DIME)_3Yb][Co(CO)_4]_2$ (**4**)

	3	**4**
formula	$C_{26}H_{42}O_{17}Sm$	$C_{26}H_{42}O_{17}Co_2Yb$
fw	894.83	917.52
cryst color	red	yellow
space group	$P6_3$ (No. 173)	$P6_3$ (No. 173)
$a = b$, Å	11.709(2)	11.552(5)
c, Å	15.505(3)	15.428(4)
V, Å^3	1841.6	1783.1
Z	2	2
cryst dimens, mm	0.27 × 0.27 × 0.30	0.40 × 0.40 × 0.50
d_{calc}, gm cm^{-3}	1.614	1.709
μ(Mo Kα), cm^{-1}	25.30	35.78
T, °C	−45	−60
scan mode	ω–2θ	ω–2θ
data collcn limits (2θ), deg	4–55	4–50
no. unique reflecns	1435	1091
no. reflecns in refin ($>3\sigma(I)$)	1147	953
no. of variables	138	138
R_F[a]	0.016	0.066
R_{wF}[b]	0.020	0.083
k[c]	0.04	0.04

[a] $R_F = \sum||F_o| - |F_c||/\sum|F_o|$. [b] $R_{wF} = (\sum w(|F_o| - |F_c|)^2/\sum w|F_o|^2)^{1/2}$. [c] $w = (\sigma(I)^2 + (kI)^2)^{-1}$.

Table 2. Positional Parameters and Their Esd's for the Cation $[(DIME)_3Sm]^{2+}$ in $[(DIME)_3Sm][Co(CO)_4]_2$ (**3**)[a]

atom	x	y	z	B,[b] Å^2
Sm	0.667	0.333	0.500	2.572(3)
O1	0.7024(2)	0.1761(2)	0.6083(2)	4.20(6)
O2	0.8950(2)	0.3332(2)	0.5010(3)	3.77(4)
O3	0.8483(2)	0.4829(3)	0.3851(2)	3.96(6)
C1	0.6247(5)	0.1173(5)	0.6830(3)	6.3(1)
C1′	0.8203(3)	0.1670(4)	0.6082(4)	5.2(1)
C2	0.8879(4)	0.2118(4)	0.5237(4)	5.4(1)
C2′	0.9870(4)	0.4012(4)	0.4316(4)	4.9(1)
C3	0.9811(4)	0.5203(4)	0.4095(3)	4.7(1)
C3′	0.8382(4)	0.5341(5)	0.3045(3)	5.1(1)

[a] The full listing is given in the supplementary material. [b] Values for anisotropically refined atoms are given in the form of the isotropic equivalent displacement parameter defined as $(4/3)[a^2B(1,1) + b^2B(2,2) + c^2B(3,3) + ab(\cos\gamma)B(1,2) + ac(\cos\beta)B(1,3) + bc(\cos\alpha)B(2,3)]$.

(15) Pribula, C. D.; Brown, T. L. *J. Organomet. Chem.* **1974**, *71*, 415.

(16) Schussler, D. P.; Robinson, W. R.; Edgell, W. F. *Inorg. Chem.* **1974**, *13*, 153.

Table 3. Positional Parameters and Their Esd's for the Cation $[(DIME)_3Yb]^{2+}$ in $[(DIME)_3Yb][Co(CO)_4]_2$ (**4**)[a]

atom	*x*	*y*	*z*	B^b Å^2
Yb	0.667	0.333	0.500	2.33(1)
O1	0.688(1)	0.166(1)	0.611(1)	5.2(4)
O2	0.888(1)	0.335(1)	0.511(1)	4.1(3)
O3	0.838(1)	0.478(1)	0.392(1)	4.1(3)
C1	0.630(2)	0.124(2)	0.688(2)	4.9(5)
C2	0.809(2)	0.165(2)	0.609(2)	4.9(5)
C3	0.870(2)	0.198(2)	0.522(2)	9.7(8)
C4	0.981(2)	0.410(2)	0.438(2)	4.9(6)
C5	0.982(5)	0.522(3)	0.410(2)	6.5(9)
C6	0.817(3)	0.525(3)	0.305(2)	16.0(8)

[a] The full listing is given in the supplementary material. [b] Values for anisotropically refined atoms are given in the form of the isotropic equivalent displacement parameter defined as $(4/3)[a^2B(1,1) + b^2B(2,2) + c^2B(3,3) + ab(\cos\gamma)B(1,2) + ac(\cos\beta)B(1,3) + bc(\cos\alpha)B(2,3)]$.

Table 4. Selected Bond Distances (Å) and Angles (deg) and Their Esd's for $[(DIME)_3Sm]^{2+}$ in **3**

	Bond Distances		
Sm–O1	2.675(4)	C2–O2	1.426(6)
Sm–O2	2.675(3)	C2′–O2	1.447(8)
Sm–O3	2.654(4)	C2′–C3	1.471(9)
C1′–O1	1.436(6)	C3–O3	1.439(7)
C1–O1	1.420(8)	C3′–O3	1.417(8)
C1′–C2	1.48(1)		
	Bond Angles		
O1–Sm–O1′	84.8(2)	Sm–O1–C1	124.3(4)
O1–Sm–O2	59.7(2)	Sm–O1–C1′	122.5(4)
O1–Sm–O2″	139.7(1)	Sm–O2–C2	116.2(3)
O1–Sm–O2′	74.4(2)	Sm–O2–C2′	117.7(4)
O1–Sm–O3	121.7(1)	Sm–O3–C3	114.3(3)
O1–Sm–O3″	149.4(2)	Sm–O3–C3′	131.5(4)
O1–Sm–O3′	83.0(2)	C1–O1–C1′	111.8(5)
O2–Sm–O2′	120	O1–C1′–C2	109.7(5)
O2–Sm–O3	62.1(2)	C1′–C2–O2	109.0(5)
O2–Sm–O3″	137.3(2)	C2–O2–C2′	112.8(4)
O2–Sm–O3′	75.2(2)	O2–C2′–C3	108.7(5)
O3–Sm–O3′	79.8(2)	C2′–C3–O3	109.2(5)
		C3–O3–C3′	114.2(5)

Table 5. Selected Bond Distances (Å) and Angles (deg) and Their Esd's for $[(DIME)_3Yb]^{2+}$ in **4**

	Bond Distances		
Yb–O1	2.69(2)	O2–C4	1.51(2)
Yb–O2	2.55(1)	O3–C5	1.50(2)
Yb–O3	2.49(1)	O3–C6	1.51(3)
O1–C1	1.33(2)	C2–C3	1.48(3)
O1–C2	1.40(2)	C4–C5	1.36(3)
O2–C3	1.49(3)		
	Bond Angles		
O1–Yb–O1′	85.5(4)	Yb–O1–C1	128(1)
O1–Yb–O2	60.6(4)	Yb–O1–C2	116(1)
O1–Yb–O2″	136.1(5)	C1–O1–C2	110(1)
O1–Yb–O2′	69.0(4)	Yb–O2–C3	113(1)
O1–Yb–O3	125.8(3)	Yb–O2–C4	112(1)
O1–Yb–O3″	145.8(4)	C3–O2–C4	112(2)
O1–Yb–O3′	83.0(3)	Yb–O3–C5	118(1)
O2–Yb–O2′	120	Yb–O3–C6	128(1)
O2–Yb–O3	65.5(4)	C5–O3–C6	113(1)
O2–Yb–O3″	140.9(5)	O1–C2–C3	111(2)
O2–Yb–O3′	77.0(4)	O2–C3–C2	104(2)
O3–Yb–O3′	79.7(4)	O2–C4–C5	116(2)
		O3–C5–C4	105(2)

structure of $[(DIME)_3Sm]^{2+}$ (Figure 3), the nine oxygens of the three diglyme ligands are arranged in a tricapped trigonal prismatic arrangement about the Sm^{2+} ion. This ion lies on a 3-fold axis. The DIME ligands are offset from the axis. The two end oxygens of each DIME are attached to opposite top and bottom verticies of the prism, while the middle oxygen caps the rectangular face. The three oxygens of each DIME are thus attached diagonally across a long rectangular face of the triginal

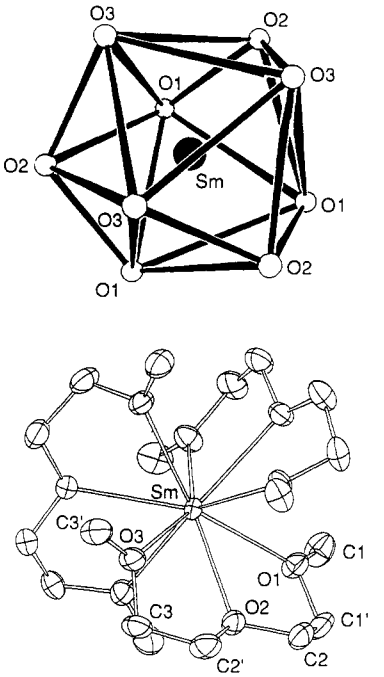

Figure 3. Structure of $[(DIME)_3Sm]^{2+}$ from **3** showing 50% thermal ellipsoids. H atoms are omitted for clarity.

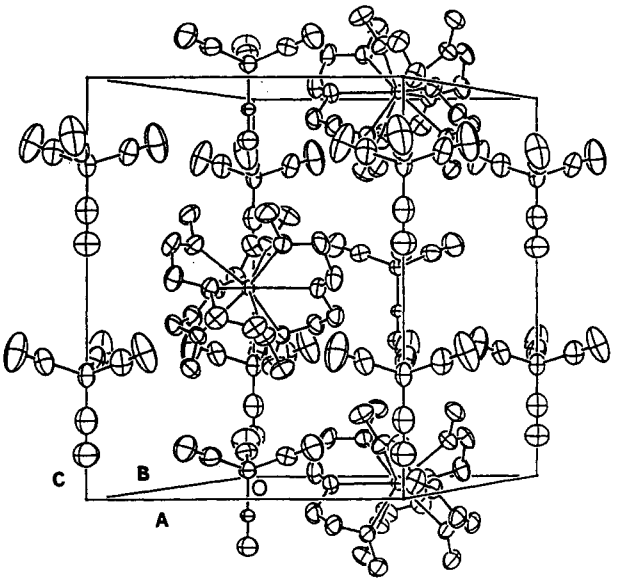

Figure 4. Lattice structure of **3** showing 50% thermal ellipsoids. H atoms are omitted for clarity.

prism. Looking down the 3-fold axis of the cation, the three DIME ligands form a three-bladed propeller configuration about the central metal.

There are two crystallographically independent carbonylate ions in the unit cell of **3**. Each carbonylate moiety has the Co and one carbonyl ligand along a 3-fold axis. One carbonylate lies on the same 3-fold axis as the Sm(II) cation, with all the colinear carbonyls pointing in the same crystallographic direction. The other carbonylate ion lies on a different 3-fold axis, with all the colinear carbonyls pointing in the same direction as the aforementioned carbonylate. A view of the lattice structure of **3** is shown in Figure 4.

The Sm–O bond distances in **3** of 2.654(4) to 2.675(4) Å are slightly longer than observed in other Sm(II) complexes. A range of 2.62(1)–2.66(1) Å for Sm–O distances is reported in $(C_5Me_5)_2Sm(THF)_2$,[17] and 2.52(1) and 2.62(2) Å distances are reported for $(C_5Me_5)_2Sm(DME)$.[18] The slight increase in the

metal–oxygen distances might be due to steric crowding around the metal center.

Although the lattice structure of **4** is isomorphous with that of **3**, the cations are slightly different. The trigonal prismatic geometry of the DIME ligands around the Yb(II) is distorted in **4**. While the Sm–O distances in **3** are virtually identical, the Yb–O distances in **4** are not: Yb–O1 = 2.69(1) Å, Yb–O2 = 2.55(1) Å, and Yb–O3 = 2.49(1) Å. Although no 9-coordinate Yb(II)–O bond lengths have been reported, the Yb–O2 and Yb–O3 bond lengths are comparable to that observed in the 7-coordinate Yb(II) complex $(C_5H_4Me)_2Yb(THF)$, 2.53(2) Å,[19] and the longest Yb–O bond in the 8-coordinate $(C_5H_5)_2Yb(DME)$, 2.50(3) Å.[20] However, the Yb–O bonds in 8-coordinate $((CH_3)_3SiC_5H_4)_2Yb(THF)_2$, 2.42(1) and 2.39(3) Å,[21] $(C_5H_5)_2Yb(DME)$, 2.45(3) Å,[20] 7-coordinate $(C_5Me_5)_2Yb(THF)$, 2.412(5) Å,[22] and $(C_2B_9H_{11})Yb(DMF)_4$, 2.37 Å,[6] and 6-coordinate $[(THF)_6Yb]^{2+}$, 2.298 Å,[6] are all substantially shorter than those observed in **4**. The observed bond lengthening occurs with increasing coordination number of the central metal.

While the variation of the Yb–O distances in **4** might reflect the fact that the X-ray data set for **4** is of lesser quality than that of **3**, this distortion might in fact be a result of steric crowding of the nine oxygens around the Yb(II) ion. Although no 9-coordinate Yb(II) ionic radius is reported, 8-coordinate Yb (1.28 Å) is *ca.* 0.12 Å smaller than Sm^{2+} (1.41 Å) and Eu^{2+} (1.39 Å).[23] The smaller size might make it more difficult for Yb(II) to accommodate nine ligands comfortably, resulting in the observed distortion in $Yb(DME)_3^{2+}$ compared to $Sm(DIME)_3^{2+}$.

As indicated in Section 3.A, the Sm complexes **3** and **5** and the Eu complex **7** are remarkably stable toward oxidation. When removed from the protection of an inert atmosphere, most Ln(II) complexes quickly change color due to oxidation of the metal to Ln(III). Red $[(DIME)_3Sm][Mn(CO)_5]_2$ and $[(DIME)_3Sm][Co(CO)_4]_2$, however only slowly turn yellow, over a period of several hours. The complex $[(DIME)_3Eu][Mn(CO)_5]_2$ changes even more slowly from a pale yellow to a colorless solid. The corresponding Yb(II) complexes on the other hand, instantaneously change from yellow-green to bright orange when removed from an inert atmosphere. These observations are of interest, since it is generally accepted that Sm(II) is more prone to oxidation than Yb(II).[24]

The difference in stabilities of the complexes toward oxidation might be related to their molecular structures. The Sm(II) complex is efficiently shielded by the three DIME ligands, as shown in Figure 3. These ligands are bound symmetrically, and present a formidable barrier toward encroachment of additional ligands, such as O_2 or other oxidants, into the Sm(II) coordination sphere. Since Eu(II) is only *ca.* 0.01 Å smaller than Sm(II),[23] and reported to have a smaller oxidation potential, it would be expected to be equally sequestered by the DIME ligands, but oxidize at an even slower rate, which is what we observe.

The $[(DIME)_3Yb]^{2+}$ complex on the other hand, has a slightly distorted arrangement of the DIME oxygens about it. This distortion might make it easier for other ligands to enter the Yb(II) coordination sphere and displace one or more DIME ligands. Such displacement could be favored due to the smaller size of the Yb(II) ion, which might favor 8-coordinate over 9-coordinate complexes. The formation of the 8-coordinate mixed ligand complexes $[(DIME)_2Yb(CH_3CN)_2]^{2+}$ in **11** and $[(DIME)Yb(CH_3CN)_5]^{2+}$ in **12** in the presence of DIME and CH_3CN ligands suggests that complexes with CN = 8 are indeed favored for Yb(II), at least with these ligands. Thus, the rapid oxidation of $[(DIME)_3Yb]^{2+}$ complexes might be related to the Yb(II) ions preference for lower coordination, which causes the 9-coordinate complex to become distorted. The distortion allows ambient O_2 to more easily reach the Yb(II) center when removed from an inert atmosphere, resulting in the observed rapid color change in these compounds.

C. Reduction of $Fe(CO)_5$ by Ytterbium Amalgam in CH_3CN and Formation of $(CH_3CN)_4Yb[Hg\{Fe(CO)_4\}_2]$ (8) and $(C_5H_5N)_4Yb[Hg\{Fe(CO)_4\}_2]$ (9). In ethers ytterbium amalgam slowly reduces $Fe(CO)_5$ to insoluble, intractable product. In CH_3CN, however, a soluble reduction product is formed: $(CH_3CN)_xYb[Hg\{Fe(CO)_4\}_2]$, (reaction 5). After removing the solvent CH_3CN, the solid product $(CH_3CN)_4Yb[Hg\{Fe(CO)_4\}_2]$ (**8**) is isolated.

$$Yb(Hg) + Fe(CO)_5 \xrightarrow{CH_3CN} (CH_3CN)_xYb[Hg\{Fe(CO)_4\}_2] + CO \quad (5)$$

$$(CH_3CN)_xYb[Hg\{Fe(CO)_4\}_2] \xrightarrow{-(x-4)CH_3CN} (CH_3CN)_4Yb[Hg\{Fe(CO)_4\}_2]$$

8

The infrared spectrum of **8** in CH_3CN [ν_{CO}, 2023 (m), 1990 (m, sh), 1974 (s), 1934 (m), 1919 (m), 1870 (vs, br) cm^{-1}] has more absorptions than that of the solvent-separated complex $[N(PPh_3)_2][Hg\{Fe(CO)_4\}_2]$ in acetone[25] [ν_{CO} 2008 (vw), 1966 (m), 1931 (s), 1855 (vs) cm^{-1}]. This indicates that the association of the Yb^{2+} ion to the counter ion $[Hg\{Fe(CO)_4\}_2]^{2-}$ is present, most likely *via* isocarbonyl linkages, and is responsible for the extra infrared absorptions at 1990 (m, sh) and 1919 (m) cm^{-1}.

Compound **8** is very soluble in pyridine. After removing all the solvents from a pyridine solution of **8**, a new complex, $(C_5H_5N)_4Yb[Hg\{Fe(CO)_4\}_2]$ (**9**), is isolated (reaction 6). The IR spectrum of **9** in CH_3CN is similar to that of **8**, suggesting similar isocarbonyl coordination to the Yb^{2+} ion.

$$(CH_3CN)_4Yb[Hg\{Fe(CO)_4\}_2] \xrightarrow{C_5H_5N} (C_5H_5N)_xYb[Hg\{Fe(CO)_4\}_2] + 4CH_3CN \quad (6)$$

$$(C_5H_5N)_xYb[Hg\{Fe(CO)_4\}_2] \xrightarrow{-(x-4)C_5H_5N} (C_5H_5N)_4Yb[Hg\{Fe(CO)_4\}_2]$$

9

Very thin needle-like crystals, presumably of the composition $(C_5H_5N)_xYb[Hg\{Fe(CO)_4\}_2]$, are grown by cooling a saturated pyridine solution of **9**. However, these needle-like crystals are too thin for single-crystal structural analysis and lose their crystallinity immediately once they leave the mother liquor.

D. Formation and Structure of $[(C_5H_5N)_5Yb(CH_3CN)_2][Hg\{Fe(CO)_4\}_2]\cdot 2C_5H_5N$ (10). Plate-like crystals of **10** are grown by cooling a saturated CH_3CN solution of $(C_5H_5N)_xYb[Hg\{Fe(CO)_4\}_2]$ (reaction 7). When dried under vacuum, **10** is converted back to **9**, quantitatively. Compounds **8**, **9**, and **10** are extremely air-sensitive in CH_3CN or pyridine solutions.

$$(C_5H_5N)_xYb[Hg\{Fe(CO)_4\}_2] \xrightarrow{C_5H_5N/CH_3CN} [(C_5H_5N)_5Yb(CH_3CN)_2][Hg\{Fe(CO)_4\}_2]\cdot 2C_5H_5N \quad (7)$$

10

(17) Evans, W. J.; Grate, J. W.; Choi, H. W.; Bloom, I.; Hunter, W. E.; Atwood, J. L. *J. Am. Chem. Soc.* **1985**, *107*, 941.
(18) Swamy, S. J.; Loebel, J.; Pickardt, J.; Schumann, H. *J. Organomet. Chem.* **1988**, *353*, 27.
(19) Zinnen, H. A.; Pluth, J. J.; Evans, W. J. *J. Chem. Soc., Chem. Commun.* **1980**, 810.
(20) Deacon, G. B.; Mackinnon, P. I.; Hambley, T. W.; Taylor, J. C. *J. Organomet. Chem.* **1983**, *259*, 91.
(21) Lappert, M. F.; Yarrow, P. I. F.; Atwood, J. L.; Shakir, R. *J. Chem. Soc. Chem. Commun.* **1980**, 987.
(22) Tilley, T. D.; Anderson, R. A.; Spencer, B.; Ruben, H.; Zalkin, A.; Templeton, D. H. *Inorg. Chem.* **1980**, *19*, 2999.
(23) Shannon, R. D. *Acta. Crystallogr.* **1976**, *A32*, 751.
(24) William J. Evans *Polyhedron* **1987**, *5*, 803.
(25) Alvarez, S.; Ferrer, M.; Reina, R.; Rossell, O.; Seco, M.; Solans, X. *J. Organomet. Chem.* **1989**, *377*, 291.

Table 6. Crystallographic Data for $[(C_5H_5N)_5Yb(CH_3CN)_2][Hg\{Fe(CO)_4\}_2]\cdot 2C_5H_5N$ (**10**), $[(DIME)_2Yb(CH_3CN)_2][Hg\{Fe(CO)_4\}_2]$ (**11**), and $[(DIME)Yb(CH_3CN)_5][B_{12}H_{12}]$ (**12**)

	10	**11**	**12**
formula	$C_{47}H_{41}Fe_2HgN_9O_8Yb$	$C_{24}H_{34}Fe_2HgN_2O_{14}Yb$	$C_6H_{41}O_3N_5B_{12}Yb$
fw	1344.74	1059.87	654.30
cryst color	red	yellow	yellow-orange
space group	$P2_1/m$ (No. 11)	$P2_12_12_1$ (No. 18)	$P2_1/n$ (No. 14)
a, Å	12.059(2)	9.576(5)	12.168(2)
b, Å	17.374(3)	15.156(3)	14.880(2)
c, Å	12.590(2)	23.918(5)	17.615(3)
β, deg	99.44(2)		97.92(1)
V, Å	2601.0	3471.2	3159.0
Z	2	4	4
cryst dimens, mm	0.20 × 0.40 × 0.40	0.35 × 0.45 × 0.50	0.22 × 0.25 × 0.30
d_{calc}, gm cm^{-3}	1.718	2.028	1.376
μ(Mo Kα), cm^{-1}	53.21	79.51	29.80
T, °C	−60	−60	−50
scan mode	ω–2θ	ω–2θ	ω–2θ
data collcn limits (2θ), deg	4–40	4–50	4–50
no. of unique reflcns	2177	4288	4798
no. of reflcns in refin ($>3\sigma(I)$)	1788	3697	3668
no. of variables	166	398	334
R_F[a]	0.107	0.040	0.037
[b]R_{wF}	0.077	0.053	0.054
k[c]	0.04	0.04	0.04

[a] $R_F = \Sigma||F_o| - |F_c||/\Sigma|F_o|$. [b] $R_{wF} = (\Sigma w(|F_o| - |F_c|)^2/\Sigma w|F_o|^2)^{1/2}$. [c] $w = (\sigma(I)^2 + (kI)^2)^{-1}$.

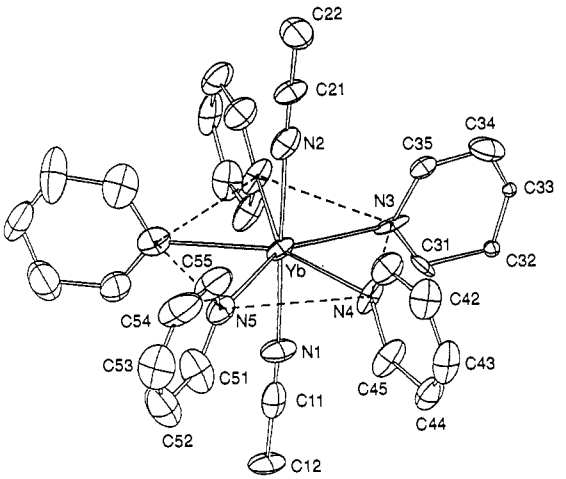

Figure 5. Molecular structure of $[(C_5H_5N)_5Yb(CH_3CN)_2]^{2+}$ from **10** showing 50% thermal ellipsoids.

While systematic absences in single crystal X-ray diffraction data from **10** are consistent with either $P2_1$ or $P2_1/m$ space groups, the structure could only be successfully refined in $P2_1/m$. Crystallographic data are given in Table 6. The structure of the cation $[(C_5H_5N)_5Yb(CH_3CN)_2]^{2+}$ is shown in Figure 5. It resides on a mirror plane which contains Yb, two axial CH_3CN ligands (N1, C11, C12, N2, C21, C22), and one C_5H_5N ligand (N3, C31–C35, and hydrogens bonded to them). In addition, two more unique pyridine ligands (N4, C41–C45, and N5, C51–C55) were located. The hydrogens of the CH_3CN ligands could not be located due to possible disordering and are therefore not included in the structure factor calculations. There are also two half-pyridines of crystallization in the asymmetric unit. The molecular plane of each pyridine is perpendicular to the mirror plane with the N atom and *para*-C atom (N6 and C63 or N7 and C73) on the mirror plane. The *para*-H atoms were not included in the structure factors calculations.

The anion $[Hg\{Fe(CO)_4\}_2]^{2-}$ resides on an inversion center. Its structure is identical to that observed in $[(THF)_2Na]_2[Hg\{Fe(CO)_4\}_2]$.[26]

Due to crystal decay during data collection and a serious absorption problem, a high quality data set was not obtained. As a result, only the metal atoms (Yb, Hg, and Fe) were refined anisotropically while the light atoms (C, O, and N) were refined isotropically. Positional parameters for the cationic complex are given in Table 7. Selected bond distances and bond angles for the cations are listed in Table 8.

The structure of the $[(C_5H_5N)_5Yb(CH_3CN)_2]^{2+}$ cation in **10** shown in Figure 5. The complex is 7-coordinate, with the ligands bound through N-atoms to Yb(II) in a pentagonal bipyramidal arrangement. The five C_5H_5N ligands are bound along each of the equatorial verticies, and the two CH_3CN ligands are bound on the apexes *trans* to each other. A crystallographic mirror plane bisects the bipyramid, and contains the two CH_3CN ligands, Yb, and one C_5H_5N. Although not crystallographically imposed,

Table 7. Positional Parameters and Their Esd's for the Cation $[(C_5H_5N)_5Yb(CH_3CN)_2]^{2+}$ in $[(C_5H_5N)_5Yb(CH_3CN)_2][Hg\{Fe(CO)_4\}_2]\cdot 2C_5H_5N$ (**10**)[a]

atom	x	y	z	B,[b] Å^2
Yb	0.7841(2)	0.250	0.5319(1)	2.75(4)
N1	0.743(3)	0.250	0.336(2)	3.8(7)*
N2	0.834(3)	0.250	0.729(2)	4.4(7)*
N3	0.991(2)	0.250	0.515(2)	2.2(6)*
N4	0.840(2)	0.390(1)	0.536(1)	3.6(5)*
N5	0.609(2)	0.332(1)	0.537(2)	5.1(6)*
C11	0.714(3)	0.250	0.240(3)	3.2(8)*
C12	0.678(4)	0.250	0.126(3)	5(1)*
C21	0.857(3)	0.250	0.818(3)	4.1(9)*
C22	0.908(4)	0.250	0.939(3)	6(1)*
C31	1.041(4)	0.250	0.417(3)	5(1)*
C32	1.155(3)	0.250	0.420(2)	1.6(6)*
C33	1.235(3)	0.250	0.517(2)	2.8(8)*
C34	1.183(3)	0.250	0.601(3)	3.7(9)*
C35	1.074(3)	0.250	0.601(3)	3.0(8)*
C41	0.865(2)	0.436(1)	0.624(2)	4.3(6)*
C42	0.880(2)	0.516(2)	0.623(2)	5.3(7)*
C43	0.876(2)	0.549(2)	0.526(2)	5.6(7)*
C44	0.851(3)	0.505(2)	0.436(2)	6.2(8)*
C45	0.844(2)	0.426(1)	0.450(2)	4.3(6)*
C51	0.541(3)	0.351(2)	0.452(2)	6.4(8)*
C52	0.445(3)	0.399(2)	0.457(3)	8.0(9)*
C53	0.428(3)	0.426(2)	0.544(2)	6.7(8)*
C54	0.499(3)	0.412(2)	0.633(2)	6.6(8)*
C55	0.592(3)	0.363(2)	0.623(2)	6.1(8)*

[a] The full listing is given in the supplementary material. Values for anisotropically refined atoms are given in the form of the isotropic equivalent displacement parameter defined as $(4/3)[a^2B(1,1) + b^2B(2,2) + c^2B(3,3) + ab(\cos\gamma)B(1,2) + ac(\cos\beta)B(1,3) + bc(\cos\alpha)B(2,3)]$. Starred values denote that were refined isotropically.

(26) Sosinsky, B. A.; Shong, R. G.; Fitzgerald, B. J.; Norem, N.; O'Rourke, C. *Inorg. Chem.* **1983**, *22*, 3124.

Table 8. Selected Bond Distances (Å) and Angles (deg) and Their Esd's for $[(C_5H_5N)_5Yb(CH_3CN)_2]^{2+}$ in **10**

Bond Distances			
Yb–N1	2.44(2)	Yb–N4	2.52(2)
Yb–N2	2.46(3)	Yb–N5	2.55(2)
Yb–N3	2.53(2)	N2–C21	1.11(4)
N1–C11	1.20(3)	N3–C35	1.35(4)
N3–C31	1.47(3)	N4–C45	1.26(2)
C21–C22	1.55(5)	C34–C35	1.31(4)
N4–C41	1.35(2)	C42–C43	1.35(3)
N5–C51	1.28(3)	C52–C53	1.25(3)
C11–C12	1.42(4)	C54–C55	1.43(3)
C33–C34	1.32(3)		
C41–C42	1.39(3)		
C43–C44	1.36(3)		
C51–C52	1.43(3)		
C53–C54	1.31(4)		
Bond Angles			
N1–Yb–N2	177.5(9)	N1–Yb–N3	87.4(7)
N1–Yb–N4	91.7(5)	N1–Yb–N5	89.6(6)
N2–Yb–N3	90.1(9)	N2–Yb–N4	87.7(4)
N2–Yb–N5	92.4(6)	N3–Yb–N4	74.9(3)
N3–Yb–N5	146.0(4)	N4–Yb–N5	71.3(5)
Yb–N1–C11	174(2)	1Yb–N2–C21	180(2)
Yb–N3–C31	128(2)	Yb–N3–C35	123(2)
Yb–N4–C41	127(1)	Yb–N4–C45	121(1)
Yb–N5–C51	123(2)	Yb–N5–C55	121(2)
N1–C11–C12	180(4)	N2–C21–C22	171(4)
N3–C31–C32	122(3)	N3–C35–C34	128(3)
N4–C41–C42	126(2)	N4–C45–C44	128(2)
N5–C51–C52	122(23)	N5–C55–C54	125(3)
C31–N3–C35	108(3)	C41–N4–C45	112(2)
C51–N5–C55	115(2)	C32–C3'3–C34	110(3)
C31–C32–C33	124(3)	C41–C42–C43	116(2)
C33–C34–C35	128(3)	C43–C44–C45	117(2)
C42–C43–C44	119(2)	C52–C53–C54	120(3)
C51–C52–C53	120(3)		
C53–C54–C55	116(2)		

the N and *para*-C atoms of the C_5H_5N ligands lie in the equatorial plane of the bipyramid. The C_5H_5N ligands themselves are perpendicular to the equatorial plane, forming a "five-bladed propeller", with the Yb and CH_3CN ligands composing the propeller shaft. This is the first example of five C_5H_5N ligands arranged in the equatorial plane of a cation. Four equatorial pyridines have been observed in the Yb(II) complex $(C_5H_5N)_4Yb[(\mu\text{-}H)_3BH]_2$,[3] the Mg(II) complex $[(C_5H_5)Mo(CO)_3]_2[(C_5H_5N)_4Mg]$,[27] and the complex $\{[(C_5H_5N)_4Na]_2[Fe_2(CO)_8]\}_\infty$.[28] Although pentagonal bipyramidal coordination geometries have been observed for the trivalent lanthanide complexes $[(THF)_5LuI_2][Co(CO)_4]$[7], and $[(THF)_5SmI_2][Co(CO)_4]$[8] and the tetravalent complexes $[LnF_7]^{3-}$ (Ln = Ce, Pr, Nd, Tb, Dy),[29] this cation represents the first example of this coordination geometry for a divalent lanthanide.

The Yb–N bond distances in **10** range from 2.52(2) to 2.55(2) Å for C_5H_5N and are slightly smaller than those observed in the Yb(II) complexes $(C_5H_5N)_4Yb[(\mu\text{-}H)_3BH]_2$, 2.566(5) and 2.579(4) Å,[3] $(C_8H_8)Yb(C_5H_5N)_3$, 2.57(1) Å,[30] and $(C_5(CH_3)_5)Yb(C_5H_5N)_2$, 2.565 Å.[31] The Yb–N distances for the CH_3CN ligands range from 2.44(2) to 2.46(3) Å. They are slightly smaller than those discussed below for **11**, **12**, and other Yb(II)–CH_3CN complexes mentioned above, which have a range of 2.510(9)–2.597(7) Å.[2,3,4] The slightly smaller Yb–N bond lengths in **10** might reflect the smaller coordination number (7) in this complex. The Yb–N–C angles in **10** of 174(2) and 180(2)° are the closest to linear for any Yb(II)–CH_3CN complex yet reported.

(27) Ulmer, S. W.; Skarstad, P. M.; Burlicht, J. M.; Hughes, R. E. *J. Am. Chem. Soc.* **1973**, *95*, 4469.
(28) Deng, H.; Shore, S. G. *Inorg. Chem.* **1992**, *31*, 2289.
(29) Sinha, S. P. *Struct. Bonding* **1976**, *25*, 69.
(30) Wayda, A. L.; Mukerji, I.; Dye, J. L.; Rogers, R. D. *Organometallics* **1987**, *6*, 1328.
(31) Tilley, T. D.; Anderson, R. A.; Brock, S.; Zalkin, A. *Inorg. Chem.* **1982**, *21*, 2647.

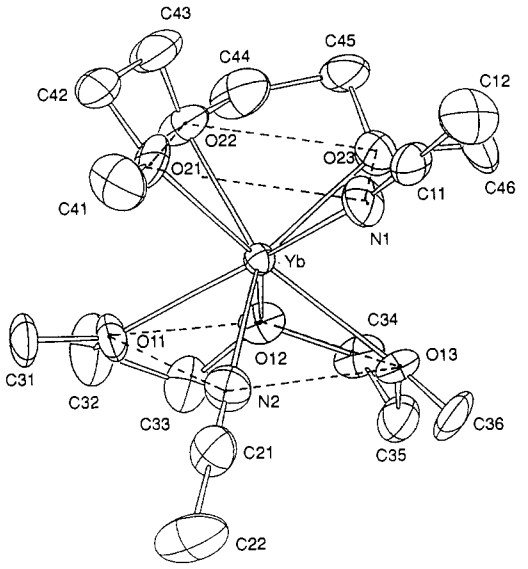

Figure 6. Structure of $[(DIME)_2Yb(CH_3CN)_2]^{2+}$ from **11** showing 50% thermal ellipsoids. H atoms are omitted for clarity.

Table 9. Positional Parameters and Their Esd's for the Cation $[(DIME)_2Yb(CH_3CN)_2]^{2+}$ in $[(DIME)_2Yb(CH_3CN)_2][Hg\{Fe(CO)_4\}_2]$ (**11**)[a]

atom	*x*	*y*	*z*	B,[b] Å^2
Yb	0.79341(5)	–0.02432(3)	0.87886(2)	1.646(7)
O11	0.866(1)	0.1029(6)	0.9351(4)	3.0(2)
O12	0.897(1)	0.0985(6)	0.8275(4)	2.7(2)
O13	0.644(1)	0.0282(7)	0.8015(4)	3.2(2)
O21	0.847(1)	–0.1116(7)	0.9638(4)	3.7(2)
O22	1.045(1)	–0.0617(7)	0.8911(4)	3.5(2)
O23	0.902(1)	–0.0980(7)	0.7975(4)	3.2(2)
N1	0.647(1)	–0.1607(8)	0.8699(5)	3.6(3)
N2	0.575(1)	0.023(1)	0.9302(5)	4.1(3)
C11	0.596(1)	–0.2285(9)	0.8635(7)	3.2(3)
C12	0.534(2)	–0.313(1)	0.8563(9)	5.0(4)
C21	0.484(2)	0.054(1)	0.9503(6)	3.8(3)
C22	0.367(2)	0.100(1)	0.9767(8)	6.0(4)
C31	0.860(2)	0.105(1)	0.9964(6)	3.8(3)
C32	0.964(2)	0.162(1)	0.9155(8)	4.7(3)
C33	0.922(2)	0.181(1)	0.8539(7)	3.7(3)
C34	0.838(2)	0.108(1)	0.7705(5)	3.4(3)
C35	0.682(2)	0.106(1)	0.7747(6)	3.5(3)
C36	0.496(1)	0.015(1)	0.7950(6)	3.9(3)
C41	0.755(3)	–0.130(1)	1.0087(6)	5.6(5)
C42	0.988(2)	–0.130(1)	0.9779(7)	4.3(4)
C43	1.065(2)	–0.139(1)	0.9247(7)	4.6(4)
C44	1.120(2)	–0.064(1)	0.8391(7)	4.7(4)
C45	1.048(2)	–0.123(1)	0.7957(6)	4.0(3)
C46	0.826(2)	–0.144(1)	0.7532(6)	4.6(4)

[a] The full listing is given in the supplementary material. Values for anisotropically refined atoms are given in the form of the isotropic equivalent displacement parameter defined as $(4/3)[a^2B(1,1) + b^2B(2,2) + c^2B(3,3) + ab(\cos\gamma)B(1,2) + ac(\cos\beta)B(1,3) + bc(\cos\alpha)B(2,3)]$.

E. Formation and Structure of $[(DIME)_2Yb(CH_3CN)_2][Hg\{Fe(CO)_4\}_2]$ (11). Complex **11** was obtained from complex **8** dissolved in a minimal amount of 1:1 DIME/CH_3CN at –40 °C (reaction 8). The space group for **11** was uniquely determined as $P2_1P2_1P2_1$.

$$(CH_3CN)_4Yb[Hg\{Fe(CO)_4\}_2] \xrightarrow{DIME/CH_3CN} [(DIME)_2Yb(CH_3CN)_2][Hg\{Fe(CO)_4\}_2] \quad (8)$$
11

The non-hydrogen atoms were refined anisotropically. The hydrogen atoms were either located or calculated as described above. The asymmetric unit contains one $[(DIME)_2Yb(CH_3CN)_2]^{2+}$ cation and one $[Hg\{Fe(CO)_4\}_2]^{2-}$ anion. Crystallographic data for **11** are listed in Table 6. Positional parameters

Table 10. Selected Bond Distances (Å) and Angles (deg) and Their Esd's for $[(DIME)_2Yb(CH_3CN)_2]^{2+}$ in **11**

Bond Distances			
Yb–O11	2.453(7)	Yb–O21	2.476(7)
Yb–O12	2.441(7)	Yb–O22	2.494(7)
Yb–O13	2.472(7)	Yb–O23	2.474(7)
Yb–N1	2.510(9)	Yb–N2	2.532(9)
O11–C31	1.47(1)	O11–C32	1.38(1)
O12–C33	1.42(1)	O12–C34	1.48(1)
O13–C35	1.39(1)	O13–C36	1.44(1)
O21–C41	1.42(2)	O21–C42	1.42(2)
O22–C43	1.43(1)	O22–C44	1.43(1)
O23–C45	1.44(1)	O23–C46	1.46(1)
N1–C11	1.15(1)	N2–C21	1.10(1)
C32–C33	1.55(2)	C34–C35	1.50(2)
C42–C43	1.48(2)	C44–C45	1.53(2)
C11–C12	1.42(2)	C21–C22	1.46(2)
Bond Angles			
O11–Yb–O12	63.9(2)	O11–Yb–O13	108.8(3)
O11–Yb–O21	84.9(3)	O11–Yb–O22	80.8(3)
O11–Yb–O23	131.9(3)	O11–Yb–N1	148.6(3)
O11–Yb–N2	75.2(3)	O12–Yb–O13	67.3(3)
O12–Yb–O21	137.4(3)	O12–Yb–O22	80.8(2)
O12–Yb–O23	77.2(3)	O12–Yb–N1	144.4(3)
O12–Yb–N2	111.2(3)	O13–Yb–O21	154.8(3)
O13–Yb–O22	136.2(3)	O13–Yb–O23	78.5(3)
O13–Yb–N1	82.9(3)	O13–Yb–N2	77.9(3)
O21–Yb–O22	65.4(3)	O21–Yb–O23	108.5(3)
O21–Yb–N1	75.3(3)	O21–Yb–N2	85.7(3)
O22–Yb–O23	65.4(3)	O22–Yb–N1	111.4(3)
O22–Yb–N2	143.8(3)	O23–Yb–N1	78.3(3)
O23–Yb–N2	149.1(3)	N1–Yb–N2	79.3(4)
Yb–O11–C31	123.4(7)	C31–O11–C32	110.8(9)
Yb–O12–C33	121.2(6)	C33–O12–C34	112.8(9)
Yb–O12–C34	112.5(7)	C35–O13–C36	109.1(9)
Yb–O13–C35	117.7(7)	C41–O21–C42	112(1)
Yb–O13–C36	127.4(7)	C43–O22–C44	114(1)
Yb–O21–C41	126.7(8)	C45–O23–C46	110(1)
Yb–O21–C42	119.9(8)	O11–C32–C33	106(1)
Yb–O22–C43	112.2(8)	O12–C33–C32	108(1)
Yb–O22–C44	112.7(7)	O12–C34–C35	108(1)
Yb–O23–C45	123.1(7)	O13–C35–C34	108(1)
Yb–O23–C46	125.2(7)	O21–C42–C43	107(1)
Yb–N1–C11	171(1)	O22–C43–C42	111(1)
Yb–N2–C21	172(1)	O22–C44–C45	112(1)
N1–C11–C12	179(1)	O23–C45–C44	105(1)
N2–C21–C22	176(2)		

for the complexes are given in Table 9 and selected bond distances and bond angles for the cations are listed in Table 10. The $[Hg\{Fe(CO)_4\}_2]^{2-}$ anion in **11** is isostructural with that in complex **10**.

The molecular structure of $[(DIME)_2Yb(CH_3CN)_2]^{2+}$ in **11** is shown in Figure 6. Yb(II) in this cation is 8-coordinate, bonded by six DIME oxygens and two CH_3CN nitrogens. The ligating atoms are arranged about the central metal in slightly distorted square antiprismatic geometry. The DIME ligands are bound in a tridentate fashion around the square bases of the antiprism, one around the top base and the other around the bottom base. The two DIME ligands are staggered with respect to each other, so that their ligating oxygens occupy all of the verticies in four of the eight triangular faces of the antiprism. The two CH_3CN ligands are bound via the nitrogens to Yb(II), occupying sites on the top and bottom bases of the antiprism. The two ligating nitrogens share an edge on one of the triangular faces.

The distortions from ideal geometry in **11** are slight but significant. The DIME ligands along each square base of the antiprism have O–O–O angles of 98(1) and 97(1)°, compared to the expected 90°, whereas the corresponding O–N–O angles are slightly compressed, both being 81(1)°. The angles on the triangular faces range from a minimum of 48(1)° for the O11–O22–O12 angle, to a maximum of 68(1)° for the O11–O22–O21 angle.

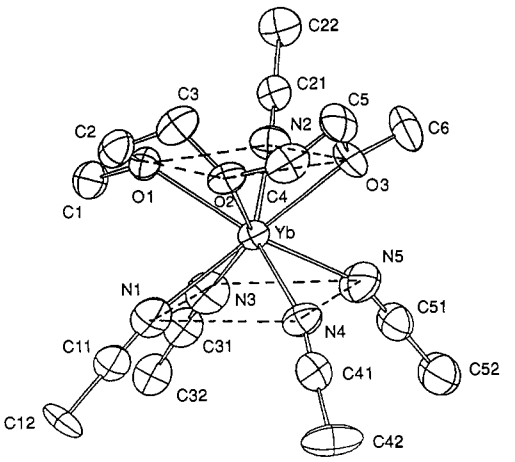

Figure 7. Structure of $[(DIME)Yb(CH_3CN)_5]^{2+}$ from **12** showing 50% thermal ellipsoids. H atoms are omitted for clarity.

Table 11. Positional Parameters and Their Esd's for the Cation $[(DIME)Yb(CH_3CN)_5]^{2+}$ in $[(DIME)Yb(CH_3CN)][B_{12}H_{12}]$ (**12**)[a]

atom	*x*	*y*	*z*	B,[b] Å^2
Yb	0.53802(3)	0.47110(2)	0.24373(2)	2.680(6)
O1	0.5323(5)	0.4420(4)	0.1028(3)	3.3(1)
O2	0.4328(5)	0.3324(4)	0.1945(3)	3.5(1)
O3	0.3366(4)	0.4625(4)	0.2711(4)	4.0(1)
N1	0.7124(7)	0.3744(5)	0.2317(4)	4.6(2)
N2	0.4448(6)	0.6057(5)	0.1736(4)	4.1(2)
N3	0.7020(7)	0.5779(6)	0.2366(5)	5.0(2)
N4	0.5707(6)	0.3717(5)	0.3600(4)	4.2(2)
N5	0.5407(7)	0.5761(6)	0.3578(5)	5.2(2)
C1	0.6204(8)	0.4802(8)	0.0660(5)	5.1(2)
C2	0.5040(8)	0.3529(7)	0.0778(5)	4.5(2)
C3	0.4036(8)	0.3263(6)	0.1138(5)	4.3(2)
C4	0.3447(8)	0.3091(7)	0.2373(6)	4.6(2)
C5	0.2694(7)	0.3881(7)	0.2417(6)	4.4(2)
C6	0.2709(8)	0.5378(8)	0.2860(6)	5.5(2)
C11	0.8018(8)	0.3492(6)	0.2362(5)	3.7(2)
C12	0.9153(7)	0.3192(7)	0.2417(6)	4.4(2)
C21	0.3907(7)	0.6518(5)	0.1348(5)	3.1(2)
C22	0.3193(8)	0.7110(6)	0.0851(6)	4.3(2)
C31	0.7855(8)	0.6111(6)	0.2391(5)	3.8(2)
C32	0.8950(8)	0.6518(6)	0.2437(5)	4.0(2)
C41	0.6184(7)	0.3389(6)	0.4115(5)	3.8(2)
C42	0.6784(9)	0.2971(7)	0.4813(6)	6.0(2)
C51	0.5755(7)	0.6103(6)	0.4123(6)	4.3(2)
C52	0.6231(9)	0.6560(8)	0.4811(6)	6.4(3)

[a] The full listing is given in the supplementary material. Values for anisotropically refined atoms are given in the form of the isotropic equivalent displacement parameter defined as $(4/3)[a^2B(1,1) + b^2B(2,2) + c^2B(3,3) + ab(\cos\gamma)B(1,2) + ac(\cos\beta)B(1,3) + bc(\cos\alpha)B(2,3)]$.

F. Formation and Structure of $[(DIME)Yb(CH_3CN)_5][B_{12}H_{12}]$ (12). Complex **12** was produced in the following metathesis reaction (reaction 9).

$$(CH_3CN)_xYbCl_2 + [(DIME)_xNa]_2[B_{12}H_{12}] \xrightarrow{CH_3CN} [(DIME)Yb(CH_3CN)_5][B_{12}H_{12}] + 2NaCl \quad (9)$$

12

The space group for **12** was uniquely determined as $P2_1/n$. Crystallographic data for **12** are given in Table 6. The non-hydrogen atoms were refined anisotropically. The hydrogen atoms were either located or calculated as described above. The asymmetric unit contains one $[(DIME)Yb(CH_3CN)_5]^{2+}$ cation and two halves of a $[B_{12}H_{12}]^{2-}$ cage (B1–B6, and B7–B12). By an inversion operation, B1–B6 generates one $[B_{12}H_{12}]^{2-}$ cage and B7–B12 generates the other. This structure of $[B_{12}H_{12}]^{2-}$ is an icosahedron in accord with a previous report of its structure.[32]

(32) Wunderlich, J. A.; Lipscomb, W. N. *J. Am. Chem. Soc.* **1960**, *82*, 4428.

Table 12. Selected Bond Distances (Å) and Angles (deg) and Their Esd's for $[(DIME)Yb(CH_3CN)_5]^{2+}$ in **12**

	Bond Distances		
Yb–O1	2.512(4)	Yb–O2	2.519(4)
Yb–O3	2.565(4)	Yb–N1	2.597(7)
Yb–N2	2.538(6)	N1–C11	1.143(8)
Yb–N3	2.568(7)	N2–C21	1.116(8)
Yb–N4	2.513(6)	N3–C31	1.125(9)
Yb–N5	2.541(6)	N4–C41	1.120(8)
N5–C51	1.117(8)	C11–C12	1.442(9)
C21–C22	1.444(9)	C31–C32	1.46(1)
C41–C42	1.478(9)	C51–C52	1.44(1)
O1–C1	1.443(8)	O1–C2	1.425(8)
C2–C3	1.50(1)	O2–C3	1.419(8)
O2–C4	1.435(9)	C4–C5	1.50(1)
O3–C5	1.429(8)	O3–C6	1.422(9)
	Bond Angles		
O1–Yb–O2	64.8(1)	Yb–O1–C1	117.1(4)
O1–Yb–O3	106.3(1)	Yb–O1–C2	116.0(4)
O1–Yb–N1	74.6(2)	C1–O1–C2	113.0(6)
O1–Yb–N2	72.8(2)	Yb–O2–C3	116.2(4)
O1–Yb–N3	88.5(2)	Yb–O2–C4	113.4(4)
O1–Yb–N4	133.2(2)	C3–O2–C4	114.1(5)
O1–Yb–N5	152.0(2)	Yb–O3–C5	119.0(4)
O2–Yb–O3	64.6(2)	Yb–O3–C6	124.8(4)
O2–Yb–N1	84.3(2)	C5–O3–C6	111.7(5)
O2–Yb–N2	107.9(2)	O1–C2–C3	106.9(5)
O2–Yb–N3	148.4(2)	O2–C3–C2	107.4(6)
O2–Yb–N4	79.3(2)	O2–C4–C5	110.2(6)
O2–Yb–N5	136.6(2)	O3–C5–C4	107.6(5)
O3–Yb–N1	143.2(2)		
O3–Yb–N2	75.9(2)	Yb–N1–C11	163.1(6)
O3–Yb–N3	144.0(2)	Yb–N2–C21	165.8(5)
O3–Yb–N4	82.3(2)	Yb–N3–C31	166.8(6)
O3–Yb–N5	77.9(2)	Yb–N4–C41	157.4(6)
N1–Yb–N2	135.5(2)	Yb–N5–C51	157.2(6)
N1–Yb–N3	71.9(2)	N1–C11–C12	178.9(8)
N1–Yb–N4	72.6(2)	N2–C21–C22	179.2(7)
N1–Yb–N5	118.9(2)	N3–C31–C32	178.3(8)
N2–Yb–N3	77.6(2)	N4–C41–C42	177.9(9)
N2–Yb–N4	150.6(2)	N5–C51–C52	177.9(9)
N2–Yb–N5	81.7(2)		
N3–Yb–N4	111.6(2)		
N3–Yb–N5	74.5(2)		
N4–Yb–N5	74.6(2)		

The structure of the $[(DIME)Yb(CH_3CN)_5]^{2+}$ in **12** is shown in Figure 7. Positional parameters are given in Table 11 and selected bond distances and bond angles are given in Table 12. Yb(II) in this cation is 8-coordinate, and the coordination geometry is likewise based on that of a slightly distorted square antiprism. The lone DIME ligand binds in a tridentate fashion around one of the bases of the antiprism. The five acetonitriles are bound through their nitrogens, and occupy all the sites on the other base of the antiprism, and one site on the base with the DIME. One triangular face has verticies composed of only ligating N atoms, while the other seven contain both O and N atoms.

Distortions from ideal geometry in **12** are like those observed in **11**. The DIME ligand along the square base of the antiprism has an O–O–O angle of 97(1)°, and the corresponding O–N–O angle is a bit compressed, being 38(1)°. The N–N–N angles on the opposite base deviate slightly from a true square, with two opposing verticies occupied by N1 and N5 at 88(1)–86(1)°, and the N3 and N4 verticies at 92(1) and 94(1)°. The angles on the triangular faces range from a minimum of 48(1)° for the O1–N1–O2 angle, to a maximum of 70(1)° for the O1–N2–N3 angle. These distortions from the ideal geometry in **11** and **12** are probably due in part to the difference in Yb–N and Yb–O bond lengths, probably because the DIME ligands may not be able to adopt 90° O–O–O angles in this geometry without a large increase in internal bond strain.

The Yb–O bond distances for the DIME ligands in $[(DIME)_2Yb(CH_3CN)_2]^{2+}$, 2.441(7) to 2.494(7) Å, are comparable to those observed in 8-coordinate Yb(II)–THF[19] and –DME[20] complexes, but are shorter than those observed in **4**. The Yb–O bonds in $[(DIME)Yb(CH_3CN)_5]^{2+}$, 2.513(6)–2.597(7) Å, however, are significantly longer than those of other 8-coordinated or lesser coordinated Yb(II) species. The bond lengths in $[(DIME)Yb(CH_3CN)_5]^{2+}$ are closer to those in 9-coordinate $[(DIME)_3Yb]^{2+}$. This bond lengthening may be due to the large number of CH_3CN ligands also coordinated to the cation in **11**. The amines may increase the electron density on the metal, causing the Yb–O bonds to lengthen.

The Yb–N bonds in **11**, 2.510(9)–2.532(9) Å, and **12**, 2.513(6)–2.597(7) Å, compare favorably with those observed in $(CH_3CN)_4Yb[(\mu\text{-}H)_3BH]_2$, 2.525(9) Å,[3] and the average length in $(CH_3CN)_6Yb[(\mu\text{-}H)_2B_{10}H_{12}]$, 2.54 Å.[4] The CH_3CN N–C–C angles are linear, but the Yb–N–C angles are slightly bent. In **11**, the Yb–N–C angles of 171(1) and 172(1)° compare well with the slight bending observed in other Yb(II)–CH_3CN complexes: $(CH_3CN)_4Yb[(\mu\text{-}H)_3BH]_2$, 170.4(4)°,[3] and $(CH_3CN)_6Yb[(\mu\text{-}H)_2B_{10}H_{12}]$, 171(2)°.[4] The Yb–N–C angles in $[(DIME)Yb(CH_3CN)_5]^{2+}$, however, ranging from 157.2(6) to 166.8(6)°, are bent considerably larger. This bending is evident in the ORTEP drawing in Figure 7.

Acknowledgment. We thank the National Science Foundation for support of this work through Grant CHE91-04035.

Supplementary Material Available: Tables of crystal data, positional parameters, anisotropic displacement parameters, bond distances, and bond angles (29 pages). Ordering information is given on any current masthead page.